



1 *Conference Proceedings Paper*

# 2 **Automated Measurement of Plant Height of Wheat** 3 **Genotypes Using A DSM Derived From UAV** 4 **Imagery**

5 **Nusret Demir**<sup>1,\*</sup>, **Namık Kemal Sönmez**<sup>1</sup>, **Taner Akar**<sup>3</sup> and **Semih Ünal**<sup>2</sup>

6 <sup>1</sup> Akdeniz University, Faculty of Science, Dept. of Space Science and Technologies, Antalya, Turkey,  
7 nusretdemir@akdeniz.edu.tr

8 <sup>2</sup> Akdeniz University, Institute of Science and Technology, Dept. of Remote Sensing and GIS, Antalya,  
9 Turkey; nksonmez@akdeniz.edu.tr

10 <sup>3</sup> Akdeniz University, Faculty of Agriculture, Dept. of Field Crops, Antalya, Turkey;  
11 tanerakar@akdeniz.edu.tr

12 \* Correspondence: nusretdemir@akdeniz.edu.tr; Tel.: +90-242-3102235

13 Published: date

14 **Abstract:** In this study, we have evaluated the use of UAV photogrammetry for monitoring of a  
15 wheat experiment under field condition, filtered DSM to derive the wheat plant heights, and  
16 compare the results with the field measurements. The images were acquired with use of low cost  
17 UAV Walkera QR350 and GoProHero3+ action camera in May 2015. Totally 477 images were  
18 acquired for quality assessment of the proposed method and a reference dataset was collected with  
19 terrestrial fieldwork. For comparison of field measurements with DSM-derived plant heights, the  
20 maximum calculated plant height in the plot was selected. The mean, median, and standard  
21 deviation were calculated as 4.66 cm, 3.75 cm., 13.78 cm. Regarding statistical t-test between the field  
22 measurements and plant heights from DSM, t-value was calculated as 1,82 and p-value was 0,071.  
23 Since t-value is larger than 0.50, the values between traditional method and our approach are highly  
24 correlated considering the fact that p-value confirms this result.

25 **Keywords:** UAV; DEM; precision agriculture; wheat experiment; plant height

---

## 27 **1. Introduction**

28 Turkey is a country with a good climate and ecological properties for agricultural production,  
29 and the agriculture occupies 24.6% workforce of the whole country[1] . Wheat production is  
30 important for Turkish economy and Turkey produced 17 million tons of wheat in 2016.

31 Traditionally, the monitoring of the wheat height is performed with field works under  
32 experiment conditions. The breeders and agronomists measure the height of the wheat genotypes  
33 with random selection in predefined interval distances. But it is time consuming and not accurate  
34 since it is not possible to measure all wheat genotypes tested in the field experiments. Thus,  
35 automated and accurate methods are needed.

36 High resolution imagery allows producing an accurate 3D model of any object including  
37 agricultural field experiments. UAV technology gives an opportunity to acquire imagery from above  
38 and then photogrammetric workflow can produce high resolution orthoimage and also a 3D model.  
39 UAV technology also allows repeating the process in predefined dates to monitor the growth of plant  
40 height of wheat genotypes periodically.

41 For monitoring of the wheat growth, the height of wheat is one of the important parameters. The  
42 monitoring of the height changes among different times will allow agronomist and breeders to  
43 determine the health and growth of the wheat experiments.

44 In the literature, crop surface models are created and used for measuring of the crop heights [2–  
45 4]. Bendig et al [3] created crop surface models of barleys with cm resolution, and they calculated a  
46 mean value for each harvest parcels to estimate the crop heights. They applied photogrammetric  
47 method with use of Agisoft Photoscan software package. Laser scanning data also were used with  
48 Tilly et al [4], they created crop surface models from the laser derived point clouds. Similarly to  
49 Bendig [3], Possoch et al [5] also generated CSM with using UAV-based crop surface model, and they  
50 used mean values of the subtracted surface model from DTM.

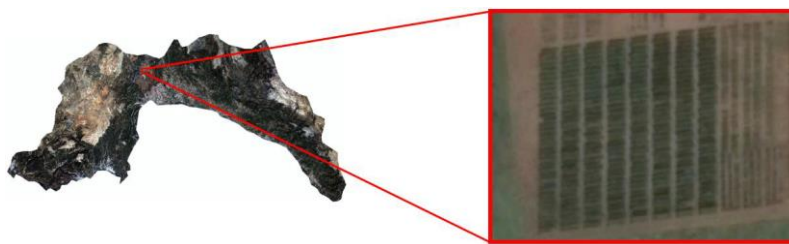
51 In agriculture, UAVs are also used for LAI and NDVI analysis to monitor the health of the crops,  
52 but without considering the height of the vegetation [6–8].

53 There are some researches regarding the tree height estimation. Considering the use of UAVs in  
54 forest inventory studies, Fritz et al. [9] detected the individual trees in an open area. They processed  
55 more than 1000 images which acquired at 55 m flying height. The used camera was a Panasonic G3  
56 with 14-42 mm focal heights and 16.6-megapixel resolution. The image acquisition was performed in  
57 April before the leaf emergence. They generated orthoimages and point clouds, and compared them  
58 with ones generated with a terrestrial laser scanner. For processing of imagery, they used CMVS and  
59 PMVS-2 software packages to process data. The processing schema consisted of 6 steps, viz. data  
60 cleaning, SIFT feature extraction, image matching, classification, point cloud generation, including  
61 camera parameters for 3D modeling of the vegetation surface. They detected 73 trees. Their study  
62 compared laser-based and image-based point clouds and confirmed that the results from image data  
63 were superior to those from the laser scanner. Feng et al. [10] classified UAV-based images to detect  
64 urban vegetation.

65 In this study, we evaluated the use of UAV photogrammetry for monitoring of the wheat field  
66 experiments and compared the results with the field measurements.

## 67 2. Experiments

68 The study area is located in Dosemealti agriculture area near Antalya province. This region has  
69 a lot of wheat cultivation sites and also industrial organizations for the process of the agricultural  
70 products. Figure 1 shows the study area which contains 192 cultivation parcels in the wheat  
71 experiments where 52 of them were investigated.



72  
73 **Figure 1.** Experimental area.

74 The process starts with image acquisition with a low cost UAV. The UAV was very simple,  
75 operated in a manual mode in high windy conditions. Therefore, the flying height varied during the  
76 acquisition.

77 The images are pre-processed due to noise elimination and enhancement. Then, commercial  
78 software package, Agisoft Photoscan was used to create high resolution orthoimage and digital  
79 surface model. For measurement of the wheat plant heights, the digital surface model was filtered to  
80 derive the terrain model. Then, the terrain model was sub-structured from the surface model. Later  
81 on, for determination of the wheat plant heights for each parcel, the maximum elevation was picked  
82 as the wheat plant height for evaluation. The results were evaluated with use of reference dataset  
83 which was created with field measurements.

84 2.1. *Image acquisition*

85 The images were acquired with use of low cost UAV Walkere QR350 and GoProHero3+ action  
86 camera on December 7th, 2015. Totally, 477 images were taken but 55 of them were selected for the  
87 process.



88

89

Figure 2 . Used UAV (left) and GoPro camera (right).

90 The reference dataset was collected with terrestrial fieldwork. A special circle with 1.5m  
91 diameter was placed above the harvest parcel and the average wheat plant height in the experimental  
92 area which intersects with the circle was reported as wheat plant height for the selected parcel.

93 2.2. *Image preprocessing*

94 The acquired images are high resolution and very useful for generating accurate surface models.  
95 But images contained noise and they were needed to be eliminated. The images contained noise  
96 because of various reasons e.g. atmospheric effects, and the sensor itself.

97 Pre-processing contains three steps; estimating the noise, noise reduction [11] Wallis filtering  
98 [12] forces the mean and the standard deviation of the image to fit given values. An adaptive edge  
99 preserving smoothing filter [11] is used for reduction of the noise. This filter preserves edge features  
100 like one-pixel line, corners, and line points.

101 2.3. *Generation of surface model and orthoimage*

102 Image orientation is a must to perform image do matching and 3D reconstruction from the  
103 preprocessed dataset. The exterior orientation was performed with automatic tie-point extraction  
104 using bundle adjustment and ground control points (measured on Google Earth imagery). Images  
105 are processed and the point cloud and orthoimage were created with the use of using Agisoft  
106 Photoscan software. The elevation of the ground control points is interpolated from ASTER based 30  
107 m resolution digital elevation model.

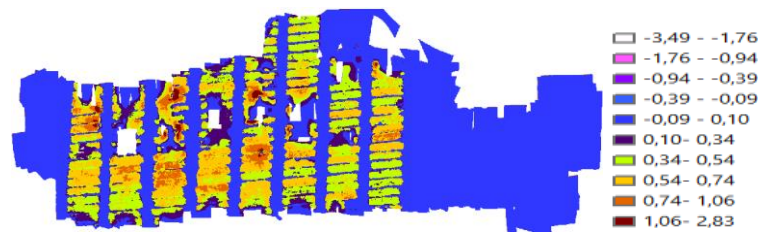
108 For calculation of wheat plant heights, terrain model has to be generated. Reduction of the  
109 generated digital surface model allows producing the terrain model. For this purpose, a progressive  
110 morphological filter method [13] is applied. The method starts with morphological opening  
111 operation on the surface model to generate a secondary surface. The elevation difference between the  
112 cells is compared with previous and the current ones during the iteration. If the difference reaches a  
113 defined threshold, the cell is classified as a non-ground object. The used threshold is calculated with  
114 a predefined slope value ( $s$ ). The window size of filtering kernel ( $dh_{T,K}$ ) has been increased, and the  
115 derived surface has been used as an input for the next operation. This is defined by Zhang et al. [13]

$$d_{h_{T,k}} = \begin{cases} dh_{max} & \text{if } d_{h_{T,k}} > dh_{max} \\ s(w_k - w_{k-1})c + d_{h_0} & \text{else if } w_k > 3 \\ dh_0 & \text{else if } w_k \leq 3 \end{cases} \quad (1)$$

116 Where is the  $d_{h_{T,k}}$  height difference threshold,  $d_{h_0}$  is the initial elevation difference threshold  
117 which approximates the error of DSM measurements,  $dh_{max}$  is the maximum elevation difference  
118 threshold (m),  $c$  is the grid size (m),  $s$  is the estimated terrain slope and  $w_k$  is the filtering window  
119 size (in number of cells) at th iteration.

120 3. Results and Discussion

121 Substruction of terrain model from the surface model gives the normalized surface model, which  
 122 will be used for calculation of the wheat plant heights in harvest parcels. The height map of the wheat  
 123 plants in the experiment is shown in Figure 3.



124

125

Figure 3. Crop Height Model

126

For comparison with the field measurements, 55 parcels have been selected.

127

For each parcel, the maximum, minimum and average height values are calculated. Since the  
 128 generated surface model is produced with the photogrammetrical method, the gaps between the  
 129 wheat parcels are also present and these gaps affect the statistical values negatively. Therefore, only  
 130 maximum height values are chosen for calculation of the wheat plant heights.

131

Wheat heights  $\mid P_i = \max(nDSM) P_i, i[1,2,3...n]$

132

For n parcels, the wheat height for the parcel n is determined as a maximum elevation in the  
 133 parcel n. There is a high correlation between the height values derived from field measurements and  
 134 the calculated values from the proposed method. The calculated statistics mean, median and standard  
 135 deviation values are listed in Table 1.

136

Table 1. Statistics of the difference between field measurements and the calculated plant  
 heights(cm)

137

Mean	Median	Std.Dev.
4.66	3.75	13.78

138

139

The mean, median, standard deviation is calculated as 4.66 cm, 3.75 cm., 13.78 cm. .Regarding  
 140 statistical t-test between the field measurements and plant heights from DSM, t-value is calculated as  
 141 1,82 and p-value are 0,071. Since t-value is larger than 0.50, the values between traditional method  
 142 and our approach are highly correlated considering the fact that p-value confirms this result. In a  
 143 previous work [14] barley heights are measured as 72.6 cm with 15.2 cm standard deviation with use  
 144 of traditional methods.

145

## 5. Conclusions

146

In this work, it is concluded that UAV imagery is effective to measure the wheat length as an  
 147 alternative method for the ground measurements. The filtering method has direct influence in the  
 148 final results. Any improvement in the filtering of surface model will allow an increase in the quality  
 149 of the results. As a future work, laser scanning can be applied to compare its performance to measure  
 150 the wheat length.

151

**Author Contributions:** Nusret Demir developed the idea and wrote the paper, Semih Unal run and  
 152 complied the experiments , Namık Kemal Sönmez contributed in processing of aerial imagery for  
 153 crop height purpose and developed the statistical methods, Taner Akar planned and conducted the  
 154 field works and contributed in the statistical analyze.

155

## Abbreviations

156

DSM:Digital Surface Model

157

nDSM:Normalized digital surface model

158

UAV:Unmanned Air Vehicle

159 **References**

- 160 1. T.C. Maliye Bakanlığı, *Yıllık Ekonomik Rapor 2016 (in Turkish)*; 2017
- 161 2. Bendig, Juliane; Bolten, Andreas; Bareth, G. UAV-based Imaging for Multi-Temporal, very high  
162 Resolution Crop Surface Models to monitor Crop Growth Variability Monitoring des  
163 Pflanzenwachstums mit Hilfe multitemporaler und hoch auflösender Oberflächenmodelle von  
164 Getreidebeständen auf Basis von Bildern. *Photogramm. - Fernerkundung - Geoinf.* **2013**, 2013.
- 165 3. Bendig, J.; Yu, K.; Aasen, H.; Bolten, A.; Bennertz, S.; Broscheit, J.; Gnyp, M. L.; Bareth, G. Combining  
166 UAV-based plant height from crop surface models, visible, and near infrared vegetation indices for  
167 biomass monitoring in barley. *Int. J. Appl. Earth Obs. Geoinf.* **2015**, 39, 79–87,  
168 doi:<https://doi.org/10.1016/j.jag.2015.02.012>.
- 169 4. Tilly, N.; Hoffmeister, D.; Cao, Q.; Huang, S.; Lenz-Wiedemann, V.; Miao, Y.; Bareth, G. Multitemporal  
170 crop surface models: accurate plant height measurement and biomass estimation with terrestrial laser  
171 scanning in paddy rice. **2014**, 8, 83623–83671.
- 172 5. Possoch, M.; Bieker, S.; Hoffmeister, D.; Bolten, A.; Schellberg, J.; Bareth, G. Multi-Temporal Crop  
173 Surface Models Combined with the RGB Vegetation Index from Uav-Based Images for Forage  
174 Monitoring in Grassland. *ISPRS - Int. Arch. Photogramm. Remote Sens. Spat. Inf. Sci.* **2016**, XLI, 991–998.
- 175 6. Lelong, C. C.; Burger, P.; Jubelin, G.; Roux, B.; Labbé, S.; Baret, F. Assessment of Unmanned Aerial  
176 Vehicles Imagery for Quantitative Monitoring of Wheat Crop in Small Plots. *Sensors* 2008, 8.
- 177 7. Sugiura, R.; Tsuda, S.; Tamiya, S.; Itoh, A.; Nishiwaki, K.; Murakami, N.; Shibuya, Y.; Hirafuji, M.; Nuske,  
178 S. Field phenotyping system for the assessment of potato late blight resistance using RGB imagery from  
179 an unmanned aerial vehicle. *Biosyst. Eng.* **2016**, 148, 1–10,  
180 doi:<https://doi.org/10.1016/j.biosystemseng.2016.04.010>.
- 181 8. Herwitz, S. R.; Johnson, L. F.; Dunagan, S. E.; Higgins, R. G.; Sullivan, D. V.; Zheng, J.; Lobitz, B. M.;  
182 Leung, J. G.; Gallmeyer, B. A.; Aoyagi, M.; Slye, R. E.; Brass, J. A. Imaging from an unmanned aerial  
183 vehicle: agricultural surveillance and decision support. *Comput. Electron. Agric.* **2004**, 44, 49–61,  
184 doi:<https://doi.org/10.1016/j.compag.2004.02.006>.
- 185 9. Fritz, A.; Kattenborn, T.; Koch, B. Uav-Based Photogrammetric Point Clouds Tree Stem Mapping In  
186 Open Stands In Comparison To Terrestrial Laser Scanner Point Clouds. *ISPRS - Int. Arch. Photogramm.*  
187 *Remote Sens. Spat. Inf. Sci.* **2013**, XL-1/W2, 141–146, doi:10.5194/isprsarchives-XL-1-W2-141-2013.
- 188 10. Feng, Q.; Liu, J.; Gong, J. UAV Remote Sensing for Urban Vegetation Mapping Using Random Forest  
189 and Texture Analysis. *Remote Sens.* 2015, 7.
- 190 11. Pateraki, M. N. *Adaptive multi-image matching for DSM generation from airborne linear array CCD data*;  
191 Gruen, P. D. A., Ed.; ETH Zurich: Zurich, 2005;
- 192 12. Wallis, H. An approach for the space variant restoration and enhancement of images. In *Symposium on*  
193 *Current Mathematical Problems in Image Science*; 1976.
- 194 13. Zhang, K.; Chen, S. C.; Whitman, D.; Shyu, M. L.; Yan, J.; Zhang, C. A progressive morphological filter  
195 for removing nonground measurements from airborne LIDAR data. *IEEE Trans. Geosci. Remote Sens.*  
196 **2003**, 41, 872–882, doi:10.1109/TGRS.2003.810682.
- 197 14. Karagöz, A.; Özbek, K.; Akar, T.; Ergün, N.; Aydoğan, S.; İsmail; Sayım Agro-Morphological Variation  
198 Among an Ancient World Barley Collection. *J. Agric. Sci.* **2017**, 23, 444–452.
- 199

© 2017 by the authors; licensee MDPI, Basel, Switzerland. This article is an open access article distributed under the terms and conditions of the Creative Commons Attribution (CC-BY) license (<http://creativecommons.org/licenses/by/4.0/>).

